Mechanics of disordered solids. III. Fracture properties

Muhammad Sahimi and Sepehr Arbabi
Department of Chemical Engineering, University of Southern California, Los Angeles, California 90089-1211
(Received 30 September 1991; revised manuscript received 6 August 1992)

Brittle fracture of disordered media are studied using Monte Carlo simulations in both two and three dimensions (3D). Elastic and superelastic percolation networks with central and bond-bending forces are used as models of disordered media. We find that the distribution of fracture strength in a solid with *broadly distributed* microscopic heterogeneities, and in *randomly reinforced* materials, is adequately described by the classical Weibull distribution, rather than the recently proposed Gumbel distribution. System-size dependence of the external stress F for fracture is also studied. We find that, contrary to recent claims, for a d-dimensional system of size L, F is given by $F \sim L^{d-1}/(\ln L)^{\psi}$, where $0 \leq \psi \leq 0.5$. The fractal dimension of the cracks is found to be about 1.7 in 2D, close to that of fracture surfaces of natural rocks at *small* scales. The scaling of the fracture stress σ_f near the percolation threshold p_c is found to obey, $\sigma_f \sim (p - p_c)^{T_f}$, where p is the fraction of intact springs (or the *damage level*) and, $T_f \simeq 2.42$ in 2D and $T_f \simeq 2.64$ in 3D. The 2D result is in agreement with the experimental estimate of T_f for fracture of thin perforated metal foils. These values are also close to the lower bound, $T_f \geq f - \nu d_{\min}$, where f is the critical exponent of the elastic moduli of the system, ν the correlation-length exponent of percolation, and $d_{\min}$ the fractal dimension of the shortest paths on a percolation cluster. Finally, we study the similarities and differences between fractured and percolation networks.

I. INTRODUCTION

In papers I and II of this series we investigated linear elastic properties of disordered media using percolation networks with central and bond-bending (BB) forces. We paid particular attention to the scaling laws that the elastic moduli of central force (CF) and BB models obey near the percolation threshold p_c, investigated the conditions under which such scaling laws may be universal, and argued that these scaling laws can provide a theoretically consistent explanation for the experimentally observed power laws for mechanical and rheological properties of a large class of disordered materials including composite solids, gel polymers, and porous rocks.

In this paper we employ elastic and superelastic percolation network to study fracture properties of disordered systems such as composite solids and natural rocks. In general, the growth of cracks and the formation of a macroscopic fracture in a disordered system is a nonequilibrium and nonlinear phenomenon. As such, the class of problems that we study in this paper is very different from those which were investigated in papers I and II. However, one main goal of this paper is to investigate whether there are any relations with or similarities between, elastic percolation networks (EPN's) studied in papers I and II and the fractured networks studied in this paper.

There already exists[1–3] an extensive literature on the general problem of mechanical failure of disordered systems. The traditional approaches of fracture mechanics to failure phenomena have certainly provided the framework for analyzing a wide variety of problems *without* considering the effect of microscopic disorder. The basis for most of these traditional approaches is the important criterion developed by Griffiths,[4] who proposed that a *single* crack becomes unstable to extension when the elastic energy released in the crack extension by a small length Δl becomes equal to the surface energy required to create a length Δl of crack surface. However, this criterion is valid for solids that are macroscopically homogeneous.

In real engineering materials, and in natural rocks, the presence of large number of flaws with various sizes, shapes, and orientations makes the problem far more complex. Disorder comes into play in many ways during a fracture process. Even small, initially present disorder can be enormously amplified during fracture. This makes fracture a collective phenomenon in which disorder plays a fundamental role. In fact, due to disorder brittle materials generally exhibit large statistical fluctuations in fracture strengths, when nominally identical samples are tested under identical loading. Because of these statistical fluctuations, it is insufficient, and indeed inappropriate, to represent the fracture behavior of a disordered material by only its *average* properties, an idea which is usually used in mean-field approaches: Fluctuations are important and must not be neglected.

In the past few years, several relatively simple network models have been introduced for both electrical[5–7] and mechanical[8] failure of disordered systems. In these models each bond of the network is supposed to describe the disordered system on a microscopic level, with failure characteristics described by a few control parameters. For example, for modeling of brittle fracture the bonds may represent the microscopic elements of a disordered solid that follow the laws of linear elasticity up to a critical threshold (e.g., in their length), beyond which they can break irreversibly and create a microscopic crack in the system. The sequence of breaking bonds and the spatial patterns they form are supposed to present a real

breaking process. Various properties of such failure phenomena have recently been investigated,[9-22] and several important features of their behavior have been discussed (see below). It is straightforward to incorporate almost any kind of disorder in such models and study its effect on the fracture properties.

In this paper we study several issues that are of fundamental importance to the fracture of disordered systems. We first describe briefly the models that we use in this paper. We then study the distribution of fracture strength (DFS) in EPN's and superelastic percolation networks (SEPN's), the stress-strain diagrams for the fracture of the elastic networks to see whether they follow universal scaling laws, and the scaling law of fracture stress σ_f at and near p_c. Finally, we compare various properties of percolation and fractured networks to see whether they share any common features.

II. PERCOLATION MODELS OF FRACTURE

We consider an $L\times L$ triangular network, or an $L\times L\times L$ cubic or bcc network with periodic boundary condition in one (2D) or two directions (3D). The boundary condition in the other direction depends on the properties of interest that we wish to calculate. Every site of the network is characterized by the displacement vector $\mathbf{u}_i=(u_{ix},u_{iy},u_{iz})$, and nearest-neighbor sites are connected by springs. We consider here the case of a brittle material for which a linear approximation is valid up to a threshold (defined below). The displacement $\mathbf{u}_i$'s are computed by minimizing the elastic energy E with respect to $\mathbf{u}_i$ given by

$$E=\frac{\alpha}{2}\sum_{\langle ij\rangle}[(\mathbf{u}_i-\mathbf{u}_j)\cdot\mathbf{R}_{ij}]^2e_{ij}+\frac{\beta}{2}\sum_{\langle jik\rangle}(\delta\theta_{jik})^2e_{ij}e_{ik}\ , \tag{1}$$

where all notations are the same as in papers I and II. Following Sahimi and Goddard,[8] three general classes of disorder can be considered. (i) Deletion or suppression of a fraction of the bonds at random or in a prescribed manner. This may represent the porosity of the system *before* the fracture process begins. Alternatively, one can designate a fraction of bonds as the rigid bonds (i.e., take $e_{ij}=\infty$ for such bonds). This would present another form of percolation effect (the SEPN's studied in papers I and II), and can be thought of as *random reinforcement* of the material in order to make it more resistive to mechanical breakdown. Various forms of such reinforcements are in fact used in practice. (ii) Random or prescribed distribution of elastic constants e of the bonds. The idea is that in real composites or rocks the shapes and sizes of the channels through which stress transport takes place are broadly distributed quantities, resulting in a different e for each channel or bond. (iii) Random or prescribed distribution of the critical thresholds. For example, each bond can be characterized by a critical displacement or length l_c, such that if it is stretched beyond l_c it breaks irreversibly. The idea is that a solid material made up intrinsically of the same material (same e everywhere) may contain regions having different resistances to breakage under an imposed external stress or potential because of, e.g., defects in manufacturing process.

We now introduce a threshold value l_c for the length of a bond, which is selected according to the probability density function

$$P(l_c)=(1-\gamma)l_c^{-\gamma}\ , \tag{2}$$

where in most cases we used $\gamma=0.8$ and $\gamma=0$ [a uniform distribution in (0,1)]. We use this power-law distribution because, unlike the uniform distribution, such power laws can give rise to unusual scaling laws for percolation networks and their universal properties,[23-25] and, therefore, we would like to see to what extent such extreme distributions can affect failure phenomena studied here. We then initiate the failure process by applying a fixed external strain (or stress) to the network in a given direction. The nodal displacements $\mathbf{u}_i$ are then determined by the same numerical methods discussed in paper I. Various failure criteria are then used (see below) to break the bonds of the network. Two different models of fracture are also employed. In model 1 only *one* bond is broken at each stage of the simulations, which is equivalent to assuming that the rate at which the elastic forces relax throughout the network is much faster than the breaking of one bond. In model 2 *all* bonds that meet the failure criterion are broken. After a spring, or a set of springs, is broken, we recalculate the nodal displacements $\mathbf{u}_i$ for the new configuration of the network, select the next spring (set of springs) to break, and so on. If the external stress or strain is not large enough to break any new spring, we gradually increase it. The simulation continues until the network finally becomes macroscopically disconnected.

III. DISTRIBUTION OF FRACTURE STRENGTHS

We define stress, or fracture strength σ_f, of a system as the lowest externally applied stress at which the system breaks down. Similar to the previous works,[8-17] we use the hypothesis that the eventual failure of the system is governed by the most critical flaw in the system, i.e., the weakest part of the system fails first. Hence, calculation of the full distribution function of fracture strength σ_f reduces to the calculation of the distribution function of the most critical flaw in the system. It can be shown that this is an excellent approximation for the failure stress of the system.

Traditionally, the Weibull distribution (WD) has been used in fitting fracture strength data. This distribution is given by

$$H(\sigma_f)=1-\exp(-cL^d\sigma_f^m)\ , \tag{3}$$

where c and m are constant, and d is the dimensionality of the system. However, Duxbury and Leath[11] formulated a new distribution which is usually referred to as the Gumbel distribution (GD), and is given by

$$H(\sigma_f)=1-\exp[-cL^d\exp(-k/\sigma_f^{\delta})]\ , \tag{4}$$

where k and δ are also constant. Equation (4) is supposed to be valid for percolating systems that are far from p_c. One can use Eqs. (3) and (4) directly to see which distri-

bution fits the data better. However, a more sensitive test of the validity of these two distributions can be made[11] if we rewrite Eqs. (3) and (4) in alternative forms. If we define a quantity A by

$$A = A_w = A_G = -\ln\left\{-\frac{\ln[1-H(\sigma_f)]}{L^d}\right\}, \tag{5}$$

then, the WD can be rewritten as

$$A_w = a_1 \ln(1/\sigma_f) + b_1 , \tag{6}$$

while the GD can be rewritten as

$$A_G = a_2(1/\sigma_f^{\delta}) + b_2 . \tag{7}$$

These two equations predict linear variations of A_w with $\ln(1/\sigma_f)$ or of A_G with $1/\sigma_f^{\delta}$. The exact value of δ has not been determined yet, but lower and upper bounds for it have been proposed.[10,11]

We first studied the DFS in a CF triangular network, both near and far from p_c. Fracture in a CF network is not only of theoretical interest, it might also be of direct relevance to mechanics of granular packings, if the friction between the packing's particles is very small. Beal and Srolowitz[16] already considered this system and computed the DFS at $p=0.9$. They found that the GD fits their data much more accurately than the WD, and that $1 \le \delta \le 2$. We used a network of $L=40$, and simulated 1000 realizations at $p=0.9$, which represents a much more extensive simulation than that of Beal and Srolowitz.[16] The threshold values l_c and the elastic constants e of the bonds were the same for all bonds, and the stretched spring whose length was *maximum* and *larger* than its l_c was broken. The distribution $H(\sigma_f)$ was found to have an almost symmetric, S-like shape. In agreement with Beal and Srolowitz, we also found that WD does not provide a very accurate fit of the simulation data, and that a GD with $\delta \simeq 2$ provides the most accurate fit of the data.

Next, we lowered p to 0.8 and simulated another 1000 realizations. The resulting $H(\sigma_f)$ is shown in Fig. 1, where it is seen that this distribution has a long tail and is very narrow. We found that neither the WD nor the GD, for any $0 \le \delta \le 2$, can fit the results accurately. If we interpret $1-p$ as the porosity of the system, we see that as the porosity of the medium increases, neither the GD nor the WD can accurately present the fracture strength data. Van den Born *et al.*,[19] who measured the mechanical strengths of highly porous ceramics, reported that the length dependence of the mechanical strength is well described by both distributions, but, for the failure pressure dependence, the GD with $\delta=1$ is more accurate. Evidently, the critical porosity (percolation threshold) of their system was very large (i.e., the percolation threshold of the solid matrix is very low), so that the porous ceramic whose strength they measured was far above its p_c. Finally, we simulated 2000 realizations at $p_{ce}^{B} \simeq 0.641$, and found that the resulting $H(\sigma_f)$ is essentially a Dirac function.

Before presenting the results with the BB model, we should discuss the above results.[26] In a percolation cluster far from p_c, there are many multiply connected paths,

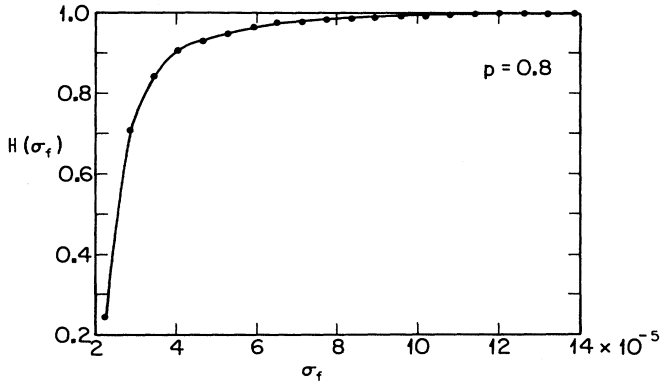

FIG. 1. Distribution of fracture strengths in a CF triangular network at $p=0.8$.

called macrolinks, which support stress transport. In such a system, the DFS may appear as a result of one or both of the following factors: (a) fluctuations of the individual characteristics of the bonds (l_c and e) in the network and, (b) fluctuations of the macrolink sizes $\mathcal{L}$ around the percolation correlation length ξ. Since in our simulations described above l_c and e were the same for all bonds, the first factor cannot contribute to the DFS. As one approaches p_c, two changes take place: First, one has fewer macrolinks and, second, the contributions of the shorter macrolinks to stress transport become negligible compared with those of the longer macrolinks. Thus, macrolink-to-macrolink fluctuations also decrease. At p_c, there is only *one* huge macrolink and, therefore, all fluctuations disappear completely and the DFS should be a Dirac function.

A network in which CF's dominate all other forces is not an adequate representation of most disordered materials, because such networks have very high percolation thresholds (see paper I), and their stress-strain diagram during fracture is not realistic, as was shown by Beale and Srolowitz.[16] Hassold and Srolowitz[16] and Yan, Lee, and Sander[16] studied fracture of a system whose elastic energy, up to the threshold l_c, was given by the Born model,

$$E = \frac{\alpha_1}{2}\sum_{\langle ij \rangle}[(\mathbf{u}_i-\mathbf{u}_j)\cdot\mathbf{R}_{ij}]^2 e_{ij} + \frac{\alpha_2}{2}\sum_{\langle ij \rangle}(\mathbf{u}_i-\mathbf{u}_j)^2 e_{ij} . \tag{8}$$

The percolation threshold of this system is the same as that of scalar percolation (see paper II). However, it is well known that this does not represent a rotationally invariant system, which makes the model unphysical for representing disordered solids. Therefore, we studied the DFS in the BB model on the triangular network which is rotationally invariant, and has not been studied before. We used an $L=60$ triangular network with $\beta/\alpha=0.1$ and $p=0.9$, and simulated 1000 realizations of the system to calculate the DFS. We found that, similar to the CF model at $p=0.9$, the DFS has an S shape. Figure 2 shows the fit of the results with the GD. In contrast with

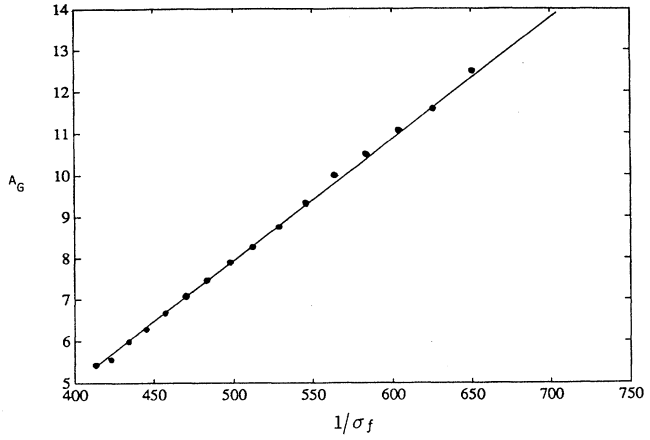

FIG. 2. Gumbel distribution fit of fracture strengths of a BB triangular network for $\beta/\alpha=0.1$, $p=0.9$, $L=60$, and $\delta=1$.

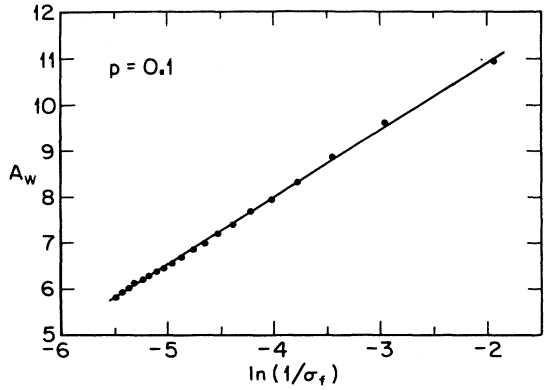

FIG. 4. Weibull distribution fit of fracture strengths of a superelastic triangular network with BB forces, for $\beta/\alpha=0.1$ and $L=40$. The fraction of rigid bonds is 0.1.

the CF case, the GD with $\delta=1$ provides the most accurate fit of the data. However, we also found that the fit of the data with the WD is only marginally worse than that of the GD, which is again in contrast with what we found for the CF case. However, when we studied the same system at $p=0.5$, the results of which are shown in Fig. 3, we found that the results can be accurately represented by the GD with $\delta=1$, while the WD provided considerably less accurate fit of the data. Thus, in contrast with the CF model, the accuracy of the fit of the results, for the BB model near p_c, with the GD becomes considerably better. Note that the $p=0.5$ network that we studied is well *below* the CF percolation threshold, which is 0.641 (see paper I).

Next we studied the DFS in a superelastic percolation network with BB forces, and determined it for three values of p, where p now refers to the fraction of rigid bonds in the network. We again used an $L=60$ network with $\beta/\alpha=1$ and simulated 1000 realizations for each p. We found that, for $p=0.1$, the WD provides an excellent fit of the data; this is shown in Fig. 4. Since in a SEPN, or in a reinforced material that can be modeled by a SEPN, there is a broad distribution of the rigidity or elastic moduli of the various islands (or clusters) of rigid and soft zones, the implication is that the WD may be more appropriate for representing the fracture strength of such materials. In contrast, we found that the GD with any $1\leq\delta\leq2$ *cannot* provide an accurate fit of the data. The best fit of the data with the GD was obtained with $\delta\simeq0.1$. However, a power law, such as $1/\sigma_f^{\delta}$ in the GD, with a very small value of the exponent, is essentially equivalent to a logarithmic law, which makes the GD with a very small value of δ essentially equivalent to the WD. Similar results were obtained with $p=0.20$. We then studied the system at $p=p_c^B=0.347$, and found the resulting $H(\sigma_f)$ to have an S shape and to be very broad. As Fig. 5 indicates, an accurate fit of the data is provided by the GD with $\delta\simeq0.5$, which is again a small value of the exponent δ. We may conclude that for a disordered material in which there is a broad distribution of elastic properties, a Weibull-like distribution, instead of the GD, can provide a better representation of the DFS.

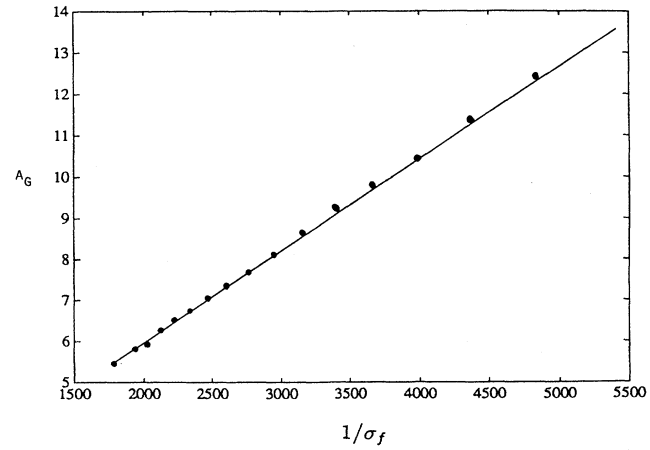

FIG. 3. Same as in Fig. 2, but at $p=0.5$.

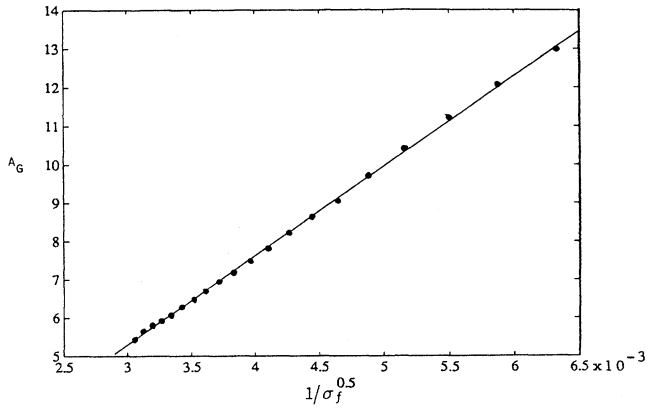

FIG. 5. Gumbel distribution fit of the results for a BB triangular network with $\beta/\alpha=0.1$ and $L=40$, using $\delta=0.5$.

IV. SCALING LAWS FOR TWO- AND THREE-DIMENSIONAL FRACTURED NETWORKS

For the simulations reported in this section, we use a slightly different failure criterion from what we used in the previous section, although the two criteria are essentially equivalent. The motivation for this is explained below. As before, we initiate the failure process by applying a fixed external strain on a fully connected network in a given direction (thus calculating the Young's modulus Y) and determining the nodal displacements $\mathbf{u}_i$. We use two different failure criteria to initiate the formation of a crack. In the first method, we select and remove that spring for which the ratio $\rho = l_m l / l_c$ is *maximum*, where l is the current length of the spring in the strained network and l_m is the maximum microscopic length of a bond in the network. In the second method, we select and remove the bond for which $U = f l_c / f_m$ is *minimum*, where f is the total microscopic force that the spring suffers, and f_m is the maximum microscopic force on a bond of the network. Both CF and BB models are used, and in the latter case both f and f_m include the BB or angle-changing forces.

We are interested in the scaling behavior of the external stress or force for breaking the network and its variations with the size of the system, since in practice this can be measured easily. This force is proportional to ρY or UY in the models with first and second failure criteria, respectively. Thus, a plot of F versus U (or ρ) would be similar to the traditional stress-strain diagrams that are measured routinely for composite solids (which is why we used these failure criteria). Instead of showing the results for each model and network size separately, we try to collapse the data for all values of L onto a single curve. Figure 6 represents the results for the BB model in the triangular network using sizes $L = 50$ and 70, and $\gamma = 0$. However, the data collapsing is not complete and, as can be seen, there are three distinct regimes. The first regime represents the initial stages of crack growth and is far from the maximum of the curve. In this regime microcracking propagates at a relatively slow rate, and is similar to a percolation process since the springs are broken essentially at random. As microcracking proceeds, one arrives in the second regime, which is in the vicinity of the maximum. In this regime microcracking is intense and the network is relatively close to macroscopic failure. Beyond the maximum, the system is in the so-called post-failure regime, and is highly sensitive to small variations in U or ρ. The qualitative features and the shapes of these curves are in perfect agreement with direct experimental measurements and observations[27,28] for various kinds of concrete and other disordered solids. To obtain quantitative information on the scaling of F with L, we assumed that

$$F \sim [L^{\Omega_1}/(\ln L)^{\psi}] h(U/L^{\Omega_1}) , \tag{9}$$

where Ω_1 and ψ are two presumably universal critical exponents, and h is a scaling function. The logarithmic term is suggested by the theoretical analyses of Duxbury, Beal, and Leath[10] and Kahng *et al.*[13] We varied both Ω_1 and ψ in order to obtain the most complete collapse of the data. We obtained

$$\Omega_1 \simeq 1 \pm 0.1 , \tag{10}$$

$$\psi \simeq 0.1 , \tag{11}$$

and found that Ω_1 and ψ are insensitive to the parameter γ of the distribution function for the critical threshold l_c, Eq. (2). In light of these results, we reanalyzed our 3D results presented previously,[17] and found that Eq. (9) can describe the data very well if we take

$$\Omega_1 \simeq 2 \pm 0.1 , \tag{12}$$

$$\psi \simeq 0.2 , \tag{13}$$

which suggest that for a d-dimensional system ($d = 2, 3$)

$$F \sim [L^{d-1}/(\ln L)^{\psi}] h(U/L^{d-1}) . \tag{14}$$

Our 3D results were obtained with very small networks (the largest size used was $L = 12$). Recent simulations of van den Born[29] using 3D CF networks with sizes up to $L = 32$ also agree with Eq. (14). Note that Eq. (14) has a simple interpretation: L^{d-1} is the surface area on which the stress F is exerted, and $(\ln L)^{\psi}$ is just the manifestation of size effects on the fracture process.

We also looked at the variations of F with N_c, the number of broken springs during the fracture process. Figure 7 shows the results for the BB model in the triangular network, where we have attempted to collapse the data for $L = 50$ and 70 onto a single curve. If we assume that

$$F \sim L^{\Omega_2} g(N_c/L^{\Omega_3}) , \tag{15}$$

we find that the most complete collapse of the data is provided by

$$\Omega_2 \simeq 1 \pm 0.05 , \tag{16}$$

$$\Omega_3 \simeq 1.7 \pm 0.1 . \tag{17}$$

The value of Ω_2 is in complete agreement with Eq. (14), as it must be. Note that Ω_3 represents the fractal dimen-

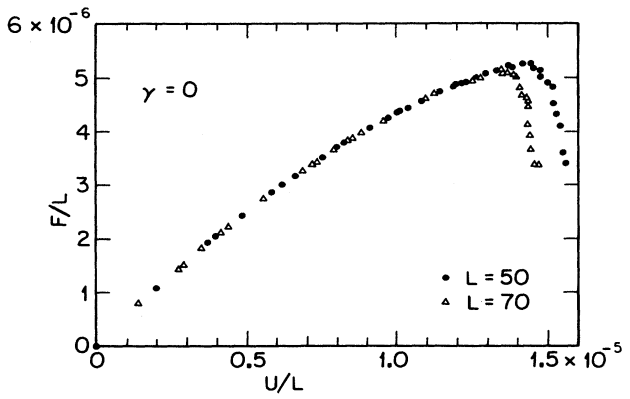

FIG. 6. Collapse of stress-strain data in the fractured triangular network with BB forces for sizes $L = 50$ and 70.

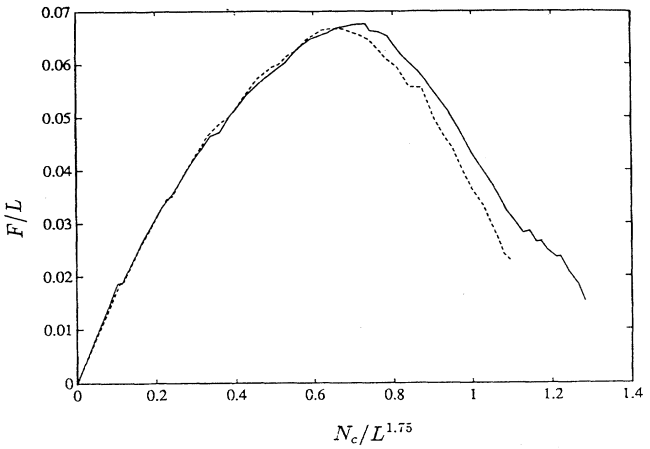

FIG. 7. Collapse of stress-strain data in the fractured triangular network with BB forces for sizes $L=50$ and 70. N_c is the number of broken bonds.

sion of *all* cracks formed in the network. If we calculate the fractal dimension of the sample-spanning fracture, we find it to be about 1.2. This value of Ω_3 agrees with the fractal dimension of 2D diffusion-limited aggregates (DLA's). However, we believe that this agreement is fortuitous, since there is no relation between the DLA model and our models. On the other hand, our result for Ω_3 is consistent with that of fracture surfaces of rocks at *small* scales, in the range 1.6–1.7.[30]

We should mention here the results of de Arcangelis *et al.*,[15] who also studied fracture of 2D solids using a lattice of beams (instead of springs used here). These authors suggested that $\Omega_1 \simeq \Omega_2 \simeq 0.75$ and $\Omega_3 \simeq 1.7$. Their value of Ω_3 is in complete agreement with ours, but when we reanalyzed their data we found that their results can be fitted more accurately with Eq. (14). Therefore, we believe that Eq. (14) provides accurate representation of the currently available simulation data.

V. SCALING OF FRACTURE STRESS NEAR THE PERCOLATION THRESHOLD

We now study the scaling of fracture strength (or stress) σ_f in a percolating system near p_c. The motivation for this study is the experimental works of Benguigui, Ron, and Bergman[20] and Sieradzki and Li.[21] In their experiments, Benguigui, Ron, and Beigman[20] measured the strain and stress of a perforated metal foil (a 2D system) and of a 2D diluted elastic network near p_c. Two different techniques were used. In the first method, the strain was increased monotonically and continuously until the system failed macroscopically, whereas in the second method stress was increased monotonically. They found that in both tests the fracture stress σ_f vanished according to a power law

$$\sigma_f \sim (p - p_c)^{T_f} , \tag{18}$$

where T_f is a new critical exponent which they found to be

$$T_f \simeq 2.5 \pm 0.4 , \tag{19}$$

and, therefore, T_f is not identical with the elasticity exponent f estimated in papers I and II. Sieradzki and Li[21] measured the fracture stress of a system composed of a 2-mm thick plate of aluminum with holes punched at positions corresponding to a triangular network of 21 rows and 20 columns. The fracture stress was determined by obtaining the full load-displacement curve for the sample to failure. They obtained $T_f \simeq 1.7 \pm 0.1$, which is much lower than that of Benguigui, Ron, and Bergman.[20] This low value of T_f is presumably because of the fact that they did not measure σ_f in the critical region close to p_c. A glance at their results shows that the measurement points were too far from p_c. Moreover, their sample size was too small, giving rise to significant size effects.

We carried out Monte Carlo simulations using triangular and simple-cubic networks with central and BB forces to see if these models of fracture can reproduce the measured value of T_f. Equation (18) can be written in the form $\sigma_f \sim \xi^{-\hat{T}_f}$, where ξ is the correlation length of percolation and $\hat{T}_f = T_f/\nu$, with ν being the critical exponent of ξ. Thus, similar to our analysis in paper I and II, we can use finite-size scaling method to estimate $\hat{T}_f$. The simulations were done at $p_c^B = 0.347$ for the triangular network and at $p_c^B \simeq 0.249$ for the simple-cubic network. The statistics of our simulations are given in Table I. We used

$$\sigma_f \sim L^{-\hat{T}_f}[a_1 + a_2 g_1(L) + a_3 g_2(L)] , \tag{20}$$

to fit our data and estimate $\hat{T}_f$. Similar to our analyses in I and II, we found that $g_1(L) = (\ln L)^{-1}$ and $g_2(L) = L^{-1}$ provide the most accurate fit of the data. Figure 8 shows the results for the triangular network, from which we obtain $\hat{T}_f = T_f/\nu \simeq 1.82 \pm 0.14$, which, together with $\nu(d=2) = \frac{4}{3}$, yield

$$T_f \simeq 2.42 \pm 0.14 . \tag{21}$$

TABLE I. Number of realizations for each network-sized L for calculating the critical exponent T_f [see Eq. (18)] at the percolation threshold.

L	20	25	30	35	40	45	50
Triangular	1000	800	600	600	600	600	600
L	6	9	12	15	18	20	
Cubic	600	450	240	120	100	50	

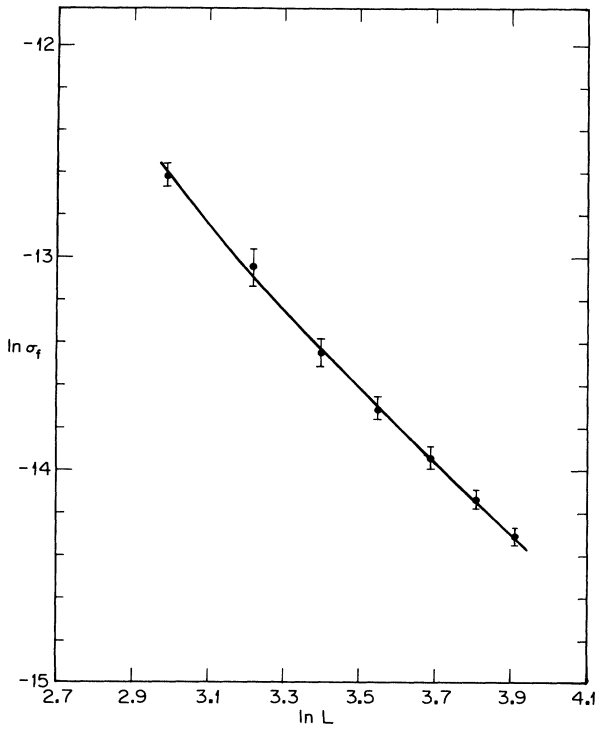

FIG. 8. Variations of fracture stress σ_f, at the bond percolation threshold of a BB triangular network of size L.

This is in good agreement with the result of Benguigui, Ron, and Bergman.[20] For the cubic network we obtained $\hat{T}_f = T_f/\nu \simeq 3 \pm 0.3$, which, together with $\nu(d=3) \simeq 0.88$, yields

$$T_f \simeq 2.64 \pm 0.3 \ . \tag{22}$$

In addition to the experimental result of Benguigui, Ron and Bergman,[20] there are also some theoretical formulae and bounds for T_f, relating it to the percolation exponents studied in papers I and II. Roy and Chakrabarti[22] proposed a lower bound for T_f based on the node-link-blob model of percolation backbones near p_c (see paper II). They proposed that

$$T_f \geq [f + (d - d_{\rm BB})\nu]/2 \ , \tag{23}$$

where $d_{\rm BB}$ is the fractal dimension of percolation backbones. This implies that

$$T_f(d=2) \geq 2.12 \ , \tag{24}$$

$$T_f(d=3) \geq 2.42 \ , \tag{25}$$

both of which agree with our results. Sharper upper and lower bounds for T_f were proposed by Bergman,[31] who suggested that

$$f - \nu d_{\rm min} \leq T_f \leq f - 1 \ , \tag{26}$$

where $d_{\rm min}$ is the fractal dimension of the shortest paths, or the chemical paths, on the backbone. These bounds, together with,[32] $d_{\rm min}(d=2) \simeq 1.13$, and $d_{\rm min}(d=3) \simeq 1.34$, predict that

$$2.45 \leq T_f(d=2) \leq 2.96 \ , \tag{27}$$

$$2.58 \leq T_f(d=3) \leq 2.76 \ , \tag{28}$$

which again agree with our results. Moreover, for both the triangular and cubic networks, our results are close to the lower bound of Bergman and, therefore, the relation $T_f = f - \nu d_{\rm min}$, cannot be ruled out.

VI. COMPARISON OF PERCOLATION AND FRACTURED NETWORKS

The last issue that we would like to address in this paper is the relation between fractured and percolation networks. In general, the growth of cracks in a disordered solid is a nonequilibrium and nonlinear phenomenon. Moreover, the growth of microcracks in a solid is *not* usually at random, but is dependent upon the stress or strain field around the cracks. On the other hand, static and linear properties of disordered solids are usually modeled by percolation networks whose bonds are cut *at random* to mimic the effect of microporosity of the solid matrix. Percolation phenomena usually represent second-order phase transitions, whereas many fracture phenomena which are studied here or take place in nature resemble first-order phase transitions. However, under certain experimental conditions the accumulation of damage and the growth of cracks can take place essentially at random as in, e.g., a solid which is under rapid thermal cycling, or a system in which the heterogeneities are broadly distributed,[30] e.g., reservoir rocks, in which case a percolation process may be able to describe the phenomenon. Therefore, it is important to know the extent of similarities between the two phenomena. If there are similarities between the two, then, percolation phenomena, which are now well understood and much easier to study, may help us to gain a deeper understanding of fracture of disordered solids and natural rocks.

There are two ways of comparing a fractured network with a percolating network. The first method is based on comparing the force distributions (FD's) and their moments in the two networks. Figure 9(a) shows the FD during a fracture process in the triangular network in the BB model after a few of bonds are broken, with $\gamma = 0$, $\beta/\alpha = 0.01$, and $L = 50$, using 50 different realizations. The fraction of the remaining bonds is $r = 0.985$, and the fracture process is modeled according to model 1 discussed above, i.e., only one bond is broken at each stage of the simulation. Figure 9(b) shows the FD in the same triangular network in which a fraction $1 - r = 0.015$ of the bonds have been removed *at random*, i.e., according to the percolation algorithm. The qualitative features of the two FD's are completely similar. Figure 10(a) shows the FD in the same fractured network in which 90% of the bonds have remained intact. At this point, the network is at about half the distance between its macroscopic failure point, which is at about $r \simeq 0.81$, and its fully connected state ($r = 1$). Figure 10(b) shows the FD in the percolating triangular network at $p = 0.7$, which is also at about half the distance between its bond percolation

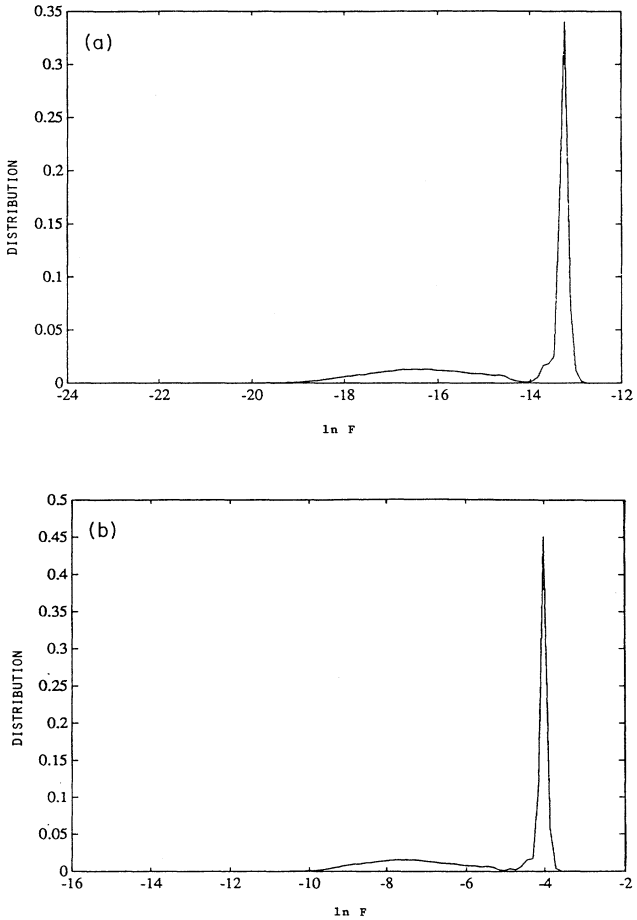

FIG. 9. Force distribution in a fractured and a percolation triangular network with BB forces with $\gamma=0$, $\beta/\alpha=0.01$, and $L=50$. (a) The fractured network at a damage level of 0.015. (b) The percolation network in which a fraction 0.015 of the bonds have been removed at random.

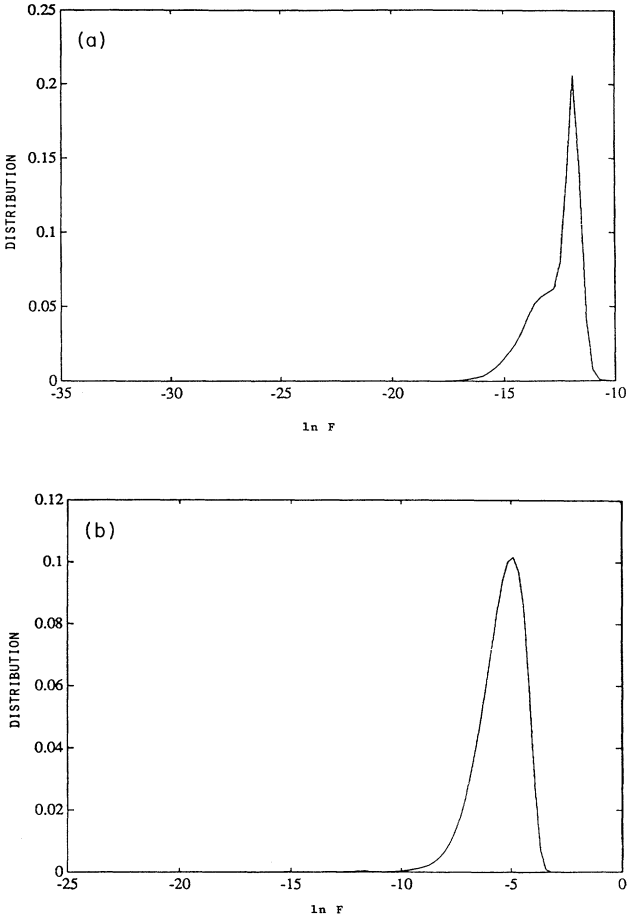

FIG. 10. Force distribution in a fractured and a percolation triangular network with BB forces with $\gamma=0$. $\beta/\alpha=0.01$, and $L=50$. (a) The fractured network at a damage level of 0.1. (b) The percolation network in which a fraction 0.3 of the bonds have been removed at random.

threshold $p_c^B=0.347$ and $p=1$. At this point, qualitative differences between the two processes have already manifested themselves in the two FD's. Finally, if we calculate the FD's very close to the macroscopic failure point of the network ($r\simeq 0.81$) and at p_c of the percolating network, we find that the two FD's are completely different.

Next, we used $\gamma=0.8$, and calculated again the FD's in the fractured and percolating networks, using another 50 realizations. The rest of the parameters were as before. Figure 11 shows the results at $r=0.7$, which should be compared with the FD of the percolating network at $p=0.7$, shown in Fig. 10(b). In this case, the two FD's are qualitatively similar. Both are unimodal and very broad. Increasing γ makes $P(l_c)$, the distribution of threshold values l_c, broader. As a result, more bonds are broken before the network fails macroscopically, and the fracture process resembles more closely a percolation phenomenon. However, when we calculated the FD very close to the macroscopic failure point of the fractured network ($r\simeq 0.58$), we found it again to be very different from that of the percolation network at p_c^B.

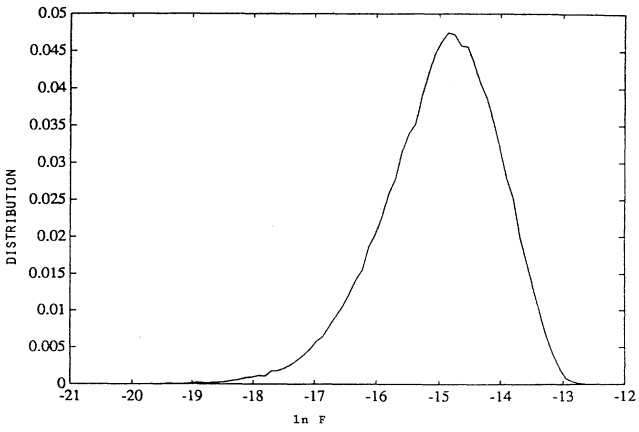

FIG. 11. Force distribution in the fractured triangular network with BB forces, with $\gamma=0.8$, $\beta/\alpha=0.01$, and $L=50$, at a damage level of 0.3. Compare this with Fig. 10(b).

These results show that, regardless of the value of γ (or the broadness of disorder distribution), the initial stages of fracture and percolation processes are very similar. That is, during the initial stages of the fracture process, the bonds that are broken according to any failure criterion are distributed essentially at random in the network. In these initial stages, the stress enhancement at the tip of a given microcrack is not strong enough to ensure that the next bond that break would be at the tip of this microcrack. However, as more microcracks nucleate, the effect of stress enhancement becomes stronger, and the deviation from a random percolation process increases. Beyond a certain point in the growth of the cracks, there will be no similarities between the two processes. Increasing γ only enhances and extends the similarities between fracture and percolation processes. In fact, in the limit $\gamma=1$, i.e., the limit of a highly heterogeneous system in which the bonds of the network are *infinitely* weak, we expect the two processes to be essentially identical. This was already suggested in "model III" of Sahimi and Goddard,[8] although the similarities and differences between the two phenomena were not quantified. Roux *et al.*[33] suggested the same, but they also did not provide quantitative information.

Given these similarities and differences between fracture and percolation processes, one would naturally be interested to locate the point at which a fracture process may start to deviate from a percolation phenomenon. The key clue is already provided in the stress-strain diagrams discussed above. Equations (9), (14), and (15) are statements of finite-size scaling which, as discussed above, can represent the fracture data up to the maximum of the stress, but beyond which the results for various network sizes cannot be collapsed onto a single curve, and finite-size scaling breaks down. This finite-size scaling is also valid for percolation networks for *any* p in the interval $p_c \leq p \leq 1$ (as long as $L < \xi$), albeit with different exponents and scaling functions. Therefore, in the type of disordered networks we study here, i.e., those that are *microscopically* disordered but *macroscopically* homogeneous, fracture and percolation processes are completely similar up to the maximum in the stress-strain diagram of the fractured system, i.e., in the regime in which finite-size scaling is valid for the fractured networks, but they will not be similar beyond this point.

The second method of comparing fracture and percolation processes is based on the values of the ratios of various elastic moduli of the two systems. It has been suggested that[34–36] for EPN's the ratio C_{11}/μ takes on a universal value at p_c, independent of the microscopic properties of the system (see paper II). We have determined[37] such ratios for our fractured networks with both models 1 and 2 and have found that, consistent with experimental data on fractured rocks,[37] they are indeed universal at the macroscopic fracture point, but their value at this point, which we have found to be about $\frac{5}{4}$ for 2D networks, is completely different from that of percolation networks, which is about 3. Thus, once again one observes certain similarities between the two phenomena, but these similarities do not extend all the way to the percolation and macroscopic failure points.

VII. SUMMARY

We studied fracture properties of disordered systems based on a number of percolation models. We found that the distribution of fracture strength in a disordered medium with broadly distributed microscopic heterogeneities is adequately described by the classical Weibull distribution, rather than the Gumbel distribution. In this sense, the Weibull distribution is more robust, and its range of applicability appears to be broader than that of the Gumbel distribution. We also studied size effects in the stress-strain diagrams during fracture processes and proposed universal scaling laws that relate fracture stress to the size of the system. Scaling behavior of fracture stress near p_c was also studied, and the appropriate critical exponents were estimated. Finally, we investigated the similarities and differences between fracture and percolation processes. We found that the extent of similarities between the two phenomena depends on the strength of disorder. If the fracturing system is *macroscopically heterogeneous,* the two phenomena are essentially identical,[30] whereas if it is *macroscopically homogeneous,* then, the two phenomena are completely similar up to the maximum in the stress-strain diagram of the fractured system, but are not similar beyond this point.

ACKNOWLEDGMENTS

This work was supported in part by the National Science Foundation Grant No. CTS 8615160, the Air Force Office of Scientific Research Grant No. 87-0284, the USC Center for Study of Fractured Reservoirs, and the San Diego Supercomputer Center. We are grateful to Karen Woo for her invaluable help in the preparation of this paper, and would like to thank Ico van den Born for discussing his results with us prior to publication. The final version of the paper was prepared while M.S. was visiting the HLRZ Supercomputer Center at KFA Jülich, Germany, and supported by the Alexander von Humboldt Foundation. He would like to thank the Center and Hans Herrmann for warm hospitality, and the Foundation for financial support.

[1] B. R. Lawn and T. R. Wilshaw, *Fracture of Brittle Solids* (Cambridge University Press, London, 1975).

[2] H. L. Ewalds and R. J. H. Wanhill, *Fracture Mechanics* (Arnold, London, 1986).

[3] *Statistical Models for the Fracture of Disordered Media,* edited by H. J. Herrmann and S. Roux (North-Holland, Amsterdam, 1990); B. K. Chakrabarti, Rev. Solid State Sci. **2**, 559 (1988).

[4] A. A. Griffiths, Philos. Trans. R. Soc. London **221**, 163 (1921).

[5] L. Niemeyer, L. Pietronero, and H. J. Wiesmann, Phys. Rev. Lett. **52**, 1023 (1984); H. J. Wiesmann and H. R. Zeller, J. Appl. Phys. **60**, 1700 (1986).

[6] H. Takayasu, Phys. Rev. Lett. **54**, 1099 (1985).

[7] L. de Arcangelis, S. Redner, and H. J. Herrmann, J. Phys. (Paris) **46**, L585 (1985).

[8]M. Sahimi and J. D. Goddard, Phys. Rev. B **33**, 7848 (1986).
[9]M. D. Stephens and M. Sahimi, Phys. Rev. B **36**, 8656 (1987).
[10]P. M. Duxbury, P. D. Beal, and P. L. Leath, Phys. Rev. Lett. **57**, 1052 (1986); Phys. Rev. B **36**, 367 (1987).
[11]P. M. Duxbury and P. L. Leath, J. Phys. A **20**, L411 (1987).
[12]Y. S. Li and P. M. Duxbury, Phys. Rev. B **40**, 4889 (1989).
[13]B. Kahng, G. G. Batrouni, S. Redner, L. de Arcangelis, and H. J. Herrmann, Phys. Rev. B **37**, 7625 (1988); D. Y. C. Chan, B. D. Hughes, L. Paterson, and C. Sirakoff, Phys. Rev. A **43**, 2905 (1991).
[14]L. de Arcangelis and H. J. Herrmann, Phys. Rev. B **39**, 2678 (1989); H. J. Herrmann, A. Hansen, and S. Roux, *ibid.* **39**, 637 (1989).
[15]L. de Arcangelis, A. Hansen, H. J. Herrmann, and S. Roux, Phys. Rev. B **40**, 877 (1989).
[16]P. D. Beale and D. J. Srolowitz, Phys. Rev. B **37**, 5500 (1988); G. N. Hassold and D. J. Srolowitz, *ibid.* **39**, 9273 (1989); H. Yan, G. Li, and L. M. Sander, Europhys. Lett. **10**, 7 (1989).
[17]S. Arbabi and M. Sahimi, Phys. Rev. B **41**, 772 (1990).
[18]W. A. Curtin and H. Scher, J. Mater. Res. **5**, 535 (1990); **5**, 554 (1990).
[19]I. C. van den Born, A. Santen, H. D. Hoekstra, and J. Th. M. De Hosson, Phys. Rev. B **43**, 3794 (1991).
[20]L. Benguigui, P. Ron, and D. J. Bergman, J. Phys. (Paris) **48**, 1547 (1987).
[21]K. Sieradzki and R. Li, Phys. Rev. Lett. **56**, 2509 (1986).
[22]P. Roy and B. K. Chakrabarti, J. Phys. C **18**, L185 (1985).
[23]P. M. Kogut and J. P. Straley, J. Phys. C **12**, 2151 (1979); A. Ben-Mizrahi and D. J. Bergman, *ibid.* **14**, 909 (1981).
[24]M. Sahimi, B. D. Hughes, L. E. Scriven, and H. T. Davis, J. Chem. Phys. **78**, 6849 (1983).
[25]B. I. Halperin, S. Feng, and P. N. Sen, Phys. Rev. Lett. **54**, 2391 (1985); S. Feng, B. I. Halperin, and P. N. Sen, Phys. Rev. B **35**, 197 (1987).
[26]D. Sornette, J. Phys. (Paris) **48**, 1843 (1987); **49**, 889 (1988); Phys. Rev. B **36**, 8847 (1987).
[27]W. F. Brace and A. S. Orange, J. Geophys. Res. **73**, 1433 (1968).
[28]J. G. M. van Mier, Mater. Constr. (Paris) **19**, 179 (1986).
[29]I. C. van den Born (unpublished).
[30]M. Sahimi, M. C. Robertson, and C. G. Sammis (unpublished).
[31]D. J. Bergman, Ann. Israel Phys. Soc. **8**, 266 (1986).
[32]H. J. Herrmann and H. E. Stanley, J. Phys. A **21**, L829 (1988).
[33]S. Roux, A. Hansen, H. J. Herrmann, and E. Guyon, J. Stat. Phys. **52**, 237 (1988).
[34]D. J. Bergman and Y. Kantor, Phys. Rev. Lett. **53**, 511 (1984).
[35]L. M. Schwartz, S. Feng, M. F. Thorpe, and P. N. Sen, Phys. Rev. B **32**, 4607 (1985).
[36]S. Arbabi and M. Sahimi, Phys. Rev. B **38**, 7173 (1988).
[37]M. Sahimi and S. Arbabi, Phys. Rev. Lett. **68**, 608 (1992).